Synthesis and Characterization of LaCu$_{0.25}$Mn$_{0.75}$O$_{3-\delta}$ Nanoparticles Perovskite Materials

Ahmed R. Arman[1], Mohamed H. Essai[2] and A.A. Ebnalwaled[1,3,*]

[1]*Electronics & Nano Devices Lab, Physics Department, Faculty of Science, South Valley University, Qena 83523, Egypt*

[2]*Electrical Engineering Department, Faculty of Engineering, Al-Azhar University, Qena 83513, Egypt*

[3]*Egypt Nanotechnology Center (EGNC), Cairo University Sheikh Zayed Campus, 12588 Giza, Egypt*

Abstract: A spongy black powder of LaCu$_{0.25}$Mn$_{0.75}$O$_{3-\delta}$ was synthesized by a modified Pechini method in this study. Properties of LaCu$_{0.25}$Mn$_{0.75}$O$_{3-\delta}$ perovskite were investigated via in situ Fourier transform infrared (FTIR) spectroscopy. X-ray diffraction results indicated obtaining highly crystalline LaCu$_{0.25}$Mn$_{0.75}$O$_{3-\delta}$ sample with crystallite size was 37 nm. FTIR results confirmed the formation of LaCu$_{0.25}$Mn$_{0.75}$O$_{3-\delta}$ nanoparticles. High-Resolution Transmission Electronic Microscope HRTEM image illustrates that the prepared sample is in the nanoscale with d-spacing equal to 0.13 nm matching the [440] plane of cubic LaCu$_{0.25}$Mn$_{0.75}$O$_{3-\delta}$. The optical properties of the obtained samples were investigated and indicated that the prepared sample is in the nanoscale.

Keywords: LaCu$_{0.25}$Mn$_{0.75}$O$_{3-\delta}$, perovskite materials, Microstrain, optical properties.

1. INTRODUCTION

Perovskite oxides appear to be among the most promising candidates for many applications [1]. In the ABO$_3$ structure of perovskite, the B cation is typically a smaller transition metal species coordinated with oxygen in octahedral position, while A is the larger cation with 12-fold coordination, and is often a rare-earth, alkaline earth, or an alkali metal [2].

Compared to stoichiometric perovskite LaMnO$_3$, oxygen deficiency-related (LaMnO$_{3-\delta}$) exhibited some specific properties, such as active oxygen mobility [3] and ion vacancy defects [4]. Indeed, this perovskite showed very promising magnetic activity and electromagnetic applications due to oxygen vacancies and cation excess which were created for LaMnO$_x$ compounds [5]. These properties can be related to different oxidation numbers of manganese (Mn^{3+} and Mn^{2+}) which exist in the crystalline structure [6].

Several previous works have been devoted to the study of electrical and magnetic properties of bulk LaMnO$_3$ materials [7-11]. The present work aims to achieve the synthesis of the novel Mn-rich perovskite oxides with La as A-site ions and Cu for B-site ions LaCu$_{0.25}$Mn$_{0.75}$O$_{3-\delta}$. These nanoparticles have been investigated by using XRD and FTIR spectroscopy. On the other hand, an attempt, regarding their optical properties has been carried out by means of

absorbance spectra measurements in terms of the optical bandgap.

2. MATERIALS AND METHOD

2.1. Synthesis of LaCu$_{0.25}$Mn$_{0.75}$O$_{3-\delta}$ Samples

The LaCu$_{0.25}$Mn$_{0.75}$O$_{3-\delta}$ polycrystalline powder was synthesized by a modified Pechini method [12]. La(NO$_3$)$_3$.H$_2$O (Alfa Aesar), Cu.H$_2$O (CH$_3$COO)$_2$ (Oxford Laboratory reagent) and C$_4$H$_6$MnO$_4$.4H$_2$O (Sigma Aldrich) were used as starting materials. Citric acid and polyethylene glycol were used as chelating agents. Lanthanum nitrate and copper acetate were preheated at 1000 ^{o}C and 200°C respectively for 10hours to eliminate moisture. Stoichiometric quantities of the above row materials were dissolved in concentrated nitric acid. Citric acid was added to the above clear solution in a molar ratio of 1:1 of citric acid: metal ions. (2g) of polyethylene glycol was dissolved in the clear solution. The obtained clear solution was kept under constant heat and vigorous stirring. Then the solution was slowly vaporized in a water bath at 85 ^{o}C overnight. Blue spongy ashes were obtained and were dried on the hot plate. The obtained black spongy ashes were put in a furnace at 900 ^{o}C for 20h to eliminate the organic matter. The resultant black powder was dry pressed using a hydraulic press, then annealed for 15h at 950°C to form pure phase, which was used for further measurements.

2.2. Characterizations

X-ray diffraction (XRD) pattern data were obtained at room temperature for powder samples of

Address correspondence to this article at the Egypt Nanotechnology Center (EGNC), Cairo University Sheikh Zayed Campus, 12588 Giza, Egypt; Tel: +201095749401; Fax: +20963211279; E-mail: kh_ebnalwaled@svu.edu.eg

LaCu$_{0.25}$Mn$_{0.75}$O$_{3-δ}$ using PANalytical diffractometer with a graphite monochromated CuKα radiation (λ = 1.54056 Å). Operating conditions were 40 kV/30 mA with an interval from 4 to 90 with step 0.06 and a scan rate of 2.5°/min. A typical Transmission Electronic Microscope (TEM) model EM-2100 High-Resolution at magnification 25 X and voltage 200 kV is employed to study the structural morphology and crystalline properties of the as-prepared powder. The functional groups that comprise the structure of the LaCu$_{0.25}$Mn$_{0.75}$O$_{3-δ}$ are evaluated using Fourier Transform Infrared (FT-IR) Spectroscopy. A typical Jasco Model 4100 – Japan with a wave number range from 400 to 4000 cm^{-1} and a resolution of 4.0 cm^{-1} is used for the current work at room temperature. A computerized SPECORD 200 PLUS analytic Jena spectrophotometer with 1 nm steps is utilized to measure the absorbance of light passing through LaCu$_{0.25}$Mn$_{0.75}$O$_{3-δ}$ nanoparticles at a wavelength (200–1100 nm). 0.001 M of LaCu$_{0.25}$Mn$_{0.75}$O$_{3-δ}$ nanoparticles was dissolved in diluted HF and was put in quarts covet for optical properties measurement.

3. RESULTS AND DISCUSSION

3.1. Phase Structure and Composition

3.1.1. X-Ray Analysis

Phase identification for the prepared LaCu$_{0.25}$Mn$_{0.75}$O$_{3-δ}$ can be obtained from the XRD pattern, which observed clearly in Figure **1**. The patterns displayed seven main peaks (200), (220), (222), (400), (422), (440), and (620) indicating that the sample was single phase LaCu$_{0.25}$Mn$_{0.75}$O$_{3-δ}$ which have a Cubic structure as reported in card No. (00-049-0807) [13].

It is obvious that the crystallites have a preferential orientation along (220) direction. It is also noteworthy
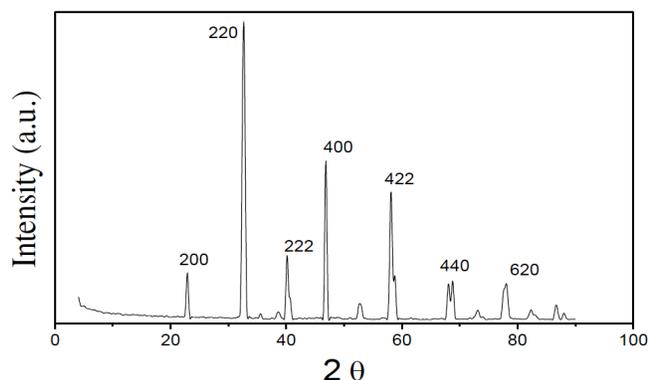

Figure 1: XRD of LaCu$_{0.25}$Mn$_{0.75}$O$_{3-δ}$.

that no peaks related to lanthanum oxide or manganese oxide are found in this spectrum, which indicates the formation of LaCu$_{0.25}$Mn$_{0.75}$O$_{3-δ}$.

Crystallite size (D) of the obtained powder was calculated from the Debye–Scherrer's formula:

$$\beta = \frac{0.94\lambda}{D\cos(\theta)} \tag{1}$$

Where β is the full width at half-maximum, D is the crystallite size, λ and θ are the wavelength of X-ray and the diffraction angle, respectively [14, 15]. From the full width at half-maximum (FWHM) (β) of the peaks, the mean square microstrain £ and the dislocation density ¥ [16, 17] of the as-prepared sample can be estimated using Eq. (2) and (3) respectively as shown in table 2

$$£ = \beta \cot\theta / 4 \tag{2}$$

$$¥ = 1/D^2 \tag{3}$$

Table **1** presents the comparison between d$_{hkl}$ for the obtained LaCu$_{0.25}$Mn$_{0.75}$O$_{3-δ}$ nanoparticles and d$_{hkl}$ for the standard Cubic LaCu$_{0.25}$Mn$_{0.75}$O$_{3-δ}$ crystals [13]. The comparison showed a good agreement with the standard crystals.

It is noted that there is a good agreement between the lattice parameters calculated values of present work and those reported elsewhere [18]. The small difference can be related to some structural defects and probably some interstitials Lanthanum or Manganese elements.

3.2. Fourier Transform Infrared (FTIR) Spectroscopy

Figure **2** shows the infrared spectra of the synthesized LaCu$_{0.25}$Mn$_{0.75}$O$_{3-δ}$ precursor powder heat-treated at 950 °C for 15 hours. The broadband in the region of 3500 cm^{-1} is related to the O-H group, which is associated with citrates and/or water molecules coordinated with the metal ions. The band positioned between 2500 and 2250 cm^{-1} was referred to the intramolecular hydrogen with C=O. A band observed at 1600 cm^{-1} is related to the C=O of acid with axial deformation. The bands observed between 1250 and 1000 cm^{-1} are ascribed to the stretching vibrations of the carboxylate (COO-) groups or C-H bonds.

The spectrum did not show any characteristic band of organic compounds in a range from 4000 to

Table 1:   Relative Intensity and Comparison between d_{hkl} for the Obtained $LaCu_{0.25}Mn_{0.75}O_{3-\delta}$ Nanocrystals and d_{hkl} for the Standard Cubic $LaCu_{0.25}Mn_{0.75}O_{3-\delta}$ Crystals

Hkl	d_{hkl}(nm) calculated	d_{hkl}(nm) for standard $LaCu_{0.25}Mn_{0.75}O_{3-\delta}$	Relative intensity (%)
200	0.388332	0.3892	13
220	0.27382	0.2752	100
222	0.224852	0.2247	16
400	0.19398	0.19455	30
422	0.158796	0.15891	40
440	0.137857	0.13758	15
620	0.12318	0.12307	14

**Table 2:   Microstructural and Optical Parameters for the Prepared $LaCu_{0.25}Mn_{0.75}O_{3-\delta}$**

Crystal size(D) (nm)	*dislocation density ¥ (× 10^4 nm^2)*	Microstrain (£) X10^-3	Lattice Parameters measured (a) (Å)	Standard Lattice Parameters (Å)	Crystal system	Energy band gap (eV)
37.1	7.27	4.454	7.77	7.7837	Cubic	3.43

$500 \ cm^{-1}$. Accordingly, the strong band observed at 600 cm^{-1}, which was ascribed to the metal-oxygen bond, indicates the formation of the corresponding oxides.
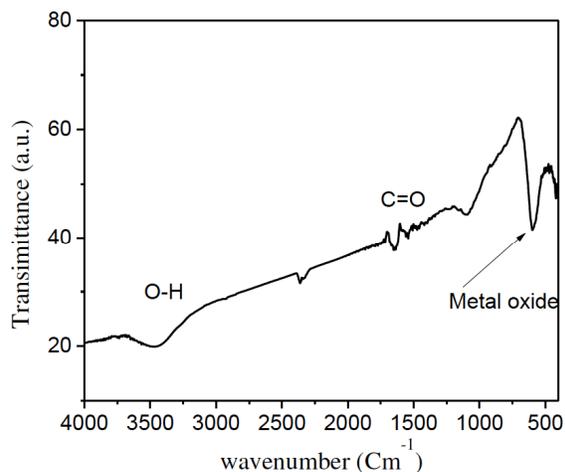

Figure 2: FTIR spectra for the different molar ratio of $LaCu_{0.25}Mn_{0.75}O_{3-\delta}$.

3.3. Morphology

HRTEM was utilized to obtain direct information about the shape and the size of the produced $LaCu_{0.25}Mn_{0.75}O_{3-\delta}$ nanoparticles. Figure **3a**) presents a typical HRTEM image for the prepared sample, from the figures it is obvious that the prepared sample is on the nanoscale. The visible lattice fringes with a d-spacing of 0.13 nm matching the [440] plane of cubic $LaCu_{0.25}Mn_{0.75}O_{3-\delta}$ Figure **3b**)
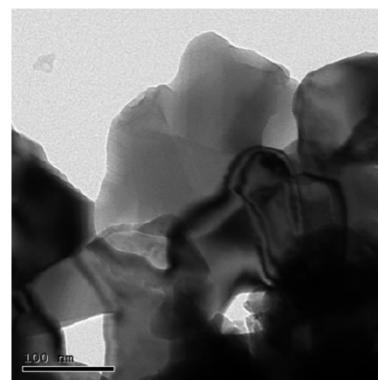
(a)
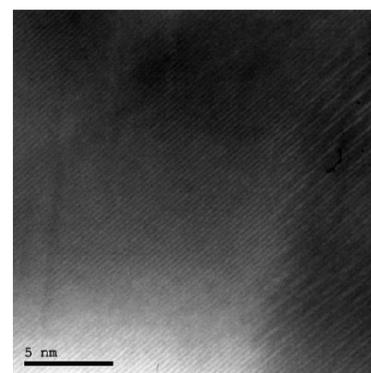
(b)

Figure 3: HRTEM of $LaCu_{0.25}Mn_{0.75}O_{3-\delta}$.

4. OPTICAL PROPERTIES

Studying the absorption spectra is considering as the simplest and direct method for investigating the band structure of the material. Figure **4** shows the

absorbance as a function of the wavelength for the prepared LaCu$_{0.25}$Mn$_{0.75}$O$_{3-\delta}$ nanoparticles. It is obvious that the perovskite interacts with the incident light and show a maximum absorption at 272 nm, which confirm the nanoscale size for the prepared sample.

The direct optical band gap (*Eg*) can be determined by the Tauc equation [19].

$$\alpha h\nu = B(h\nu - Eg)^{1/2} \qquad (4)$$

Where α is the absorption coefficient, $h\nu$ is the energy of the incident photon and B is a constant depends on the transition probability.

As shown in Figure **5** the obtained optical band gap for LaCu$_{0.25}$Mn$_{0.75}$O$_{3-\delta}$ nanoparticles is 3.43 eV.
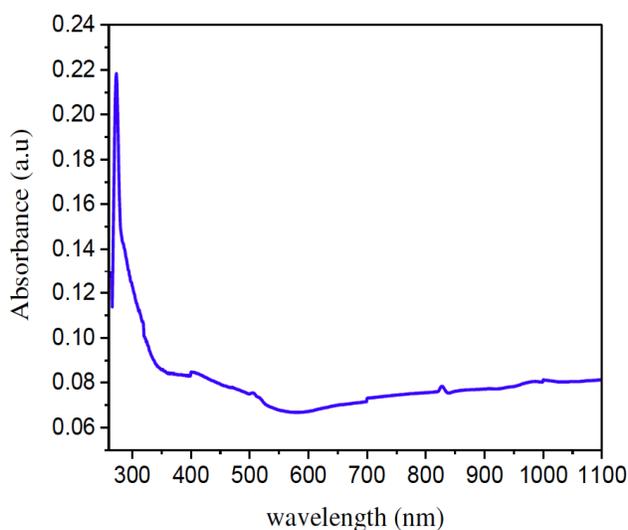
Figure 4: Absorbance spectra for the different molar ratio of LaCu$_{0.25}$Mn$_{0.75}$O$_{3-\delta}$.
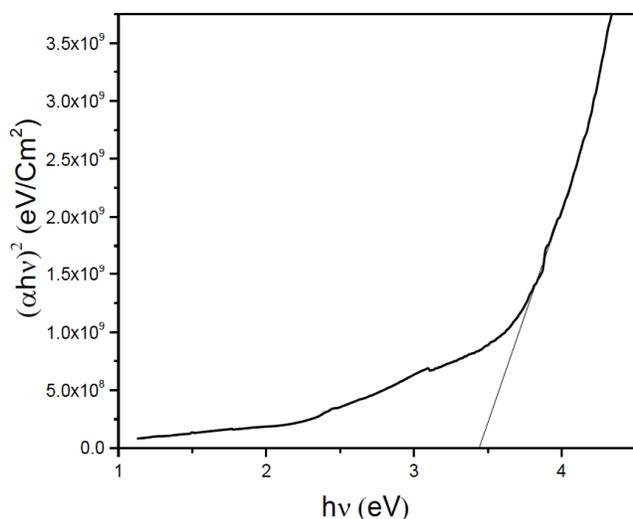
Figure 5: The plots of $\alpha h\nu^2$ versus ($h\nu$) of LaCu$_{0.25}$Mn$_{0.75}$O$_{3-\delta}$.

CONCLUSION

LaCu$_{0.25}$Mn$_{0.75}$O$_{3-\delta}$ nanoparticles were synthesized using a facile and effective method. The crystallinity, crystallite size and the morphology of the prepared samples are confirmed by obtaining high-quality LaCu$_{0.25}$Mn$_{0.75}$O$_{3-\delta}$ samples. The blue shift of the optical band gap confirms the nano size for the prepared LaCu$_{0.25}$Mn$_{0.75}$O$_{3-\delta}$ samples.

For future work we plan to prepare LaCu$_{0.25}$Mn$_{0.75}$O$_{3-\delta}$ nanoparticles using the same approach, but with changing the Cu/Mn ratio to investigate the effect of that on the different properties of the prepared samples. Also, we will examine the suitability of the obtained samples to work as cathode for fuel cell applications.

REFERENCES

[1]   Zhu Y, *et al*. Multiwalled carbon nanotubes beaded with ZnO nanoparticles for ultrafast nonlinear optical switching. Adv Mater 2006; 18(5): 587-592.
https://doi.org/10.1002/adma.200501918

[2]   Pena MA, Fierro JLG. Chemical structures and performance of perovskite oxides. Chem Rev 2001; 101(7): 1981-2018.
https://doi.org/10.1021/cr980129f

[3]   Spinicci R, Delmastro A, Ronchetti S, Tofanari A. Catalytic behaviour of stoichiometric and non-stoichiometric LaMnO3 perovskite towards methane combustion. Mater Chem Phys 2003; 78(2): 393-399.
https://doi.org/10.1016/S0254-0584(02)00218-3

[4]   Alonso JA, *et al*. Non-stoichiometry, structural defects and properties of LaMnO 3+ δ with high δ values (0.11≤ δ≤ 0.29). J Mater Chem 1997; 7(10): 2139-2144.
https://doi.org/10.1039/a704088a

[5]   Dezanneau G, Sin A, Roussel H, Audier M, Vincent H. Magnetic properties related to structure and complete composition analyses of nanocrystalline La1− xMn1− yO3 powders. J Solid State Chem 2003; 173(1): 216-226.
https://doi.org/10.1016/S0022-4596(03)00027-6

[6]   Vincent H, Audier M, Pignard S, Dezanneau G, Senateur JP. Crystal Structure Transformations of a Magnetoresistive La0. 8MnO3–δ Thin Film. J Solid State Chem 164(2): 2002; 177-187.
https://doi.org/10.1006/jssc.2001.9440

[7]   Bouderbala A, *et al*. Structural, magnetic and magnetocaloric study of La0. 7− xEuxSr0. 3MnO3 (x= 0.1, 0.2 and 0.3) manganites. Ceram Int 2015; 41(6): 7337-7344.
https://doi.org/10.1016/j.ceramint.2015.02.034

[8]   Yang J, *et al*. Structural, transport, and magnetic properties in the Ti-doped manganites LaMn1− xTixO3 (0≤ x≤ 0.2). Solid State Commun 2005; 136(5): 268-272.
https://doi.org/10.1016/j.ssc.2005.08.005

[9]   Bejar M, Sdiri N, Hussein M, Mazen S, Dhahri E. Magnetocaloric effect on strontium vacancies in polycrystalline La0. 7Sr0. 3− x□ xMnO3. J Magn Magn Mater 2007; 316(2): e566-e568.
https://doi.org/10.1016/j.jmmm.2007.03.022

[10]   Triki M, Dhahri E, Hlil EK. Unconventional critical magnetic behavior in the Griffiths ferromagnet La0. 4Ca0. 6MnO2. 8□ 0.2 oxide. J Solid State Chem 2013; 201: 63-67.
https://doi.org/10.1016/j.jssc.2013.02.019

[11] Sdiri N, Bejar M, Hussein M, Mazen S, Dhahri E. Effect of the oxygen deficiency in physical properties of La0. 7Ca0. 25Sr0. 05MnO3− δ☐ δ oxides (0⩽ δ⩽ 0.15). J Magn Magn Mater 2007; 316(2): e703-e706.
https://doi.org/10.1016/j.jmmm.2007.03.066

[12] Pérez-Flores JC, *et al*. A-and B-site Ordering in the A-Cation-Deficient Perovskite Series La2–x NiTiO6− δ (0≤ x< 0.20) and Evaluation as Potential Cathodes for Solid Oxide Fuel Cells. Chem Mater 2013; 25(12): 2484-2494.
https://doi.org/10.1021/cm4008014

[13] Andreson MT, Greenwood KB, Taylor GA, Poppelmeier KR. "B-cation arrangements in double perovskite. Progr Solid State Chem 1993; 22: 197-233.
https://doi.org/10.1016/0079-6786(93)90004-B

[14] Scherrer P. Bestimmung der inneren Struktur und der Größe von Kolloidteilchen mittels Röntgenstrahlen. in Kolloidchemie Ein Lehrbuch, Springer 1912; pp. 387-409.
https://doi.org/10.1007/978-3-662-33915-2_7

[15] Zhang W, *et al*. A redox reaction to synthesize nanocrystalline Cu2-x Se in aqueous solution. Inorg Chem 2000; 39(9): 1838-1839.
https://doi.org/10.1021/ic990871d

[16] Anwar S, Pattanaik M, Mishra BK, Anwar S. Effect of deposition time on lead selenide thermoelectric thin films prepared by chemical bath deposition technique. Mater Sci Semicond Process 2015; 34: 45-51.
https://doi.org/10.1016/j.mssp.2015.02.014

[17] Begum A, Hussain A, Rahman A. Effect of deposition temperature on the structural and optical properties of chemically prepared nanocrystalline lead selenide thin films. Beilstein J Nanotechnol 2012; 3(1): 438-443.
https://doi.org/10.3762/bjnano.3.50

[18] Ruiz-González ML, Cortés-Gil R, Alonso JM, Hernando A, Vallet-Regí M, González-Calbet JM. Structural ordering and ferromagnetism in La4Mn4O11. Chem Mater 2006; 18(24): 5756-5763.
https://doi.org/10.1021/cm0609193

[19] Pankove JI. Optical processes in semiconductors Prentice-Hall. New Jersey 1971; vol. 92.